Spin waves in periodically perturbed films

P. Landeros[1,*] and D. L. Mills[2]

[1]*Departamento de Física, Universidad Técnica Federico Santa María, Avenida España 1680, 2390123 Valparaíso, Chile*

[2]*Department of Physics and Astronomy, University of California, Irvine, California 92697, USA*

(Received 27 November 2011; published 22 February 2012)

We have developed a theory that describes the spin wave response of ferromagnetic films magnetized in plane whose magnetic properties have been modulated in a periodic manner. The theory is patterned after Brillouin-Wigner perturbation theory in quantum mechanics. We provide expressions for the response of the film to applied magnetic fields of frequency Ω and wave vector $\vec{k}_{\parallel}$ parallel to the surface. Our response functions form the basis for a description of the microwave response of such films, and also of Brillouin light scattering from spin waves if desired. We present a series of calculations that explore effects that may be realized in ferromagnetic resonance studies of such structures. The theory accounts for striking peaks observed recently in the frequency variation of the linewidth of periodically modulated ferromagnetic films, and provides insight into their origin. We also predict new features in the ferromagnetic resonance spectrum of periodically perturbed films.

DOI: 10.1103/PhysRevB.85.054424 PACS number(s): 75.78.−n, 75.70.−i, 76.20.+q, 85.70.Kh

I. INTRODUCTION

For over two decades, there has been great interest in the response characteristics and properties of very small magnetic structures characterized by submicron-length scales or below. One encounters new physics in these structures not present in bulk magnetic matter. Aspects of the magnetic response of such systems can be controlled or engineered in diverse ways not possible in macroscopic samples. This may be done by integrating different materials into a structure, by synthesizing interacting arrays of particles or islands, and by construction of samples with tailored geometries.

Recently there has been a focus on the magnetic response of small-scale periodic structures of diverse sorts, which are referred to as magnonic crystals. These range from periodically patterned films to two-dimensional arrays of nanospheres or disks and one-dimensional arrays of cylinders, to cite some examples. In such structures, the propagation characteristics of spin waves may be controlled and manipulated in a manner familiar from the general concepts of wave propagation in periodic structures. Gaps open up in the dispersion relation at the appropriate points in the Brillouin zone, for instance. An excellent review with emphasis on probing spin waves in periodic structures by Brillouin light scattering has been given by Gubbiotti *et al.*[1] This paper also discusses theoretical methodologies that have been employed in the description of spin wave propagation in periodic structures. We call attention to early discussions of the spin wave normal modes in periodic arrays of ferromagnetic nanospheres[2] and also one-dimensional arrays of ferromagnetic cylinders wherein the magnetizations of all cylinders are parallel.[3] Recently very interesting experimental and theoretical studies of cylindrical arrays have appeared that explore lattices of cylinders where antiparallel alignment of the magnetization is present.[4] By now we have in hand many studies of the nature of spin waves in diverse samples of periodic character.

This paper is devoted to the theory of the magnetic response of a thin film of infinite spatial extent whose properties have been varied periodically, perpendicular to an in-plane direction. We develop the theory of the response functions which can be used to describe the ferromagnetic resonance (FMR) response of the film, or if desired these can be incorporated into a discussion of the Brillouin light scattering (BLS) spectrum. While information on the dispersion relation of spin waves in such a film is embedded in the response functions (they appear as poles in the frequency plane in their denominators) these entities also provide us with line intensities and linewidths of features in the spectrum as well. Dissipation as described by the Landau-Lifshitz-Gilbert (LLG) equation is incorporated in the approach. Numerical calculations are quite straightforward to perform within our framework. The explicit expressions we obtain here for the response functions are based on a scheme equivalent to the Brillouin-Wigner perturbation theory of quantum mechanics. We use our response functions to carry out a set of theoretical studies of the FMR spectrum of an in-plane magnetized film upon whose surface a periodic array of ridges is present.

We remark that our study is motivated by experimental results presented recently by Barsukov and collaborators.[5] These authors study the dependence of the FMR linewidth of such a periodically modulated film on frequency, to find sharp peaks at a set of discrete frequencies. While much of the literature on spin waves in periodic structures has been directed toward the very interesting "magnonic bands", the data in Ref. 5 show that sharp structures in the spin damping rate may be engineered into magnetic thin films through imposition of periodic modulations of their properties. This may be very useful for applications in which one may wish to introduce large changes in the spin damping rate through small modulation in either frequency or magnetic field. Our theory provides an account of these structures, and thus provides an understanding of the physics responsible for the peaks. We shall see that in such periodically modulated films, the response falls into two categories we may describe as weak- and strong-coupling limits. The samples explored in Ref. 5 fall into the weak-coupling regime, by our classification.

We remark that some years ago, a theoretical description of two-magnon damping in thin ferromagnets was developed for in-plane magnetized films.[6] This was later extended to the case where the magnetization is tipped out of plane.[7,8] While the focus in these papers is on two-magnon damping and also two-magnon induced frequency shifts in the FMR

response, the presentations contain a description of a general formalism that may be used to describe the interaction of spin waves with static defects of diverse character. The application to two-magnon scattering by random defects is just one use of the formalism. In the present paper, this formalism is applied to a film with periodic perturbations rather than those of random character.

The organization of this paper is as follows. In Sec. II, we present the formalism we employ and in Sec. III we present a series of numerical calculations directed toward the ferromagnetic response of in-plane magnetized films whose surface is modulated in a stripelike fashion. Concluding comments are found in Sec. IV.

II. THEORY

A. Formalism

In this section we develop the theoretical structure discussed in Sec. I. We shall consider a ferromagnetic film sufficiently thin that we may ignore the variation of all quantities in the direction normal to the surfaces of the film. The magnetization will be assumed parallel to the z axis, which lies in plane, and the y axis is normal to the surfaces.

We assume that the film is exposed to an external, time-dependent magnetic field $h_\beta(\vec{r}_\parallel;t) = h_\beta(\vec{k}'_\parallel)\exp[i\vec{k}'_\parallel\cdot\vec{r}_\parallel - i\Omega t]$. The subscript $\parallel$ refers to wave vectors in the plane of the film. Of interest is the expectation value of the time-dependent, transverse component of the magnetization operator $\langle m_\alpha(\vec{r}_\parallel;t)\rangle$ induced by such an external field. In general this will have the form, in the linear response regime, $\langle m_\alpha(\vec{r}_\parallel;t)\rangle = (1/\sqrt{L^2 d})\sum_{\vec{k}_\parallel}\langle m_\alpha(\vec{k}_\parallel)\rangle\exp[i\vec{k}_\parallel\cdot\vec{r}_\parallel - i\Omega t]$ for a film of nominal thickness d that covers a plane of area $A = L^2$. The response functions of interest to us, denoted by $S_{\alpha\beta}(\vec{k}_\parallel,\vec{k}'_\parallel;\Omega)$, link the expectation value just described to the amplitude of the external driving field:

$$\langle m_\alpha(\vec{k}_\parallel)\rangle = \sum_\beta S_{\alpha\beta}(\vec{k}_\parallel,\vec{k}'_\parallel;\Omega)h_\beta(\vec{k}'_\parallel). \tag{1}$$

For a film with perfectly flat surfaces and no interior defects, we have $S_{\alpha\beta}(\vec{k}_\parallel,\vec{k}'_\parallel;\Omega) = \delta_{\vec{k}_\parallel,\vec{k}'_\parallel}\tilde{S}^0_{\alpha\beta}(\vec{k}_\parallel;\Omega)$, where[6]

$$\tilde{S}^0_{xx}(\vec{k}_\parallel;\Omega) = \frac{\gamma^2 M_S\tilde{H}_y(\vec{k}_\parallel)}{\tilde{\Omega}^2(\vec{k}_\parallel)-\Omega^2}, \tag{2a}$$

$$\tilde{S}^0_{yy}(\vec{k}_\parallel;\Omega) = \frac{\gamma^2 M_S\tilde{H}_x(\vec{k}_\parallel)}{\tilde{\Omega}^2(\vec{k}_\parallel)-\Omega^2}, \tag{2b}$$

$$\tilde{S}^0_{xy}(\vec{k}_\parallel;\Omega) = -\frac{i\gamma M_S\Omega}{\tilde{\Omega}^2(\vec{k}_\parallel)-\Omega^2}, \tag{2c}$$

$$\tilde{S}^0_{yx}(\vec{k}_\parallel;\Omega) = -\tilde{S}^0_{xy}(\vec{k}_\parallel;\Omega). \tag{2d}$$

Here γ is the gyromagnetic ratio and M_S the saturation magnetization, $\tilde{H}_{x,y}(\vec{k}_\parallel) = H_{x,y}(\vec{k}_\parallel) - i\alpha\Omega/\gamma$, where $H_x(\vec{k}_\parallel)$ and $H_y(\vec{k}_\parallel)$ are given in Eqs. (15) and (16) of Ref. 6 for films whose thickness is small compared to the wavelength of the spin waves of interest, and $\alpha = G/\gamma M_S$ where G is the Gilbert damping constant. The quantity α is the standardly defined dimensionless damping constant which enters the Landau-Lifschitz-Gilbert equation. This quantity was denoted by g in Ref. 6. Finally $\tilde{\Omega}(\vec{k}_\parallel) = \gamma[\tilde{H}_x(\vec{k}_\parallel)\tilde{H}_y(\vec{k}_\parallel)]^{1/2}$. The expressions above incorporate the dynamic dipolar fields generated by spin motions of wave vector $\vec{k}_\parallel$ in the film, as well as the influence of exchange as described macroscopically by introducing the exchange stiffness $D = 2A/M_S$.

The discussion above describes the response of the film to an external magnetic field that varies in time and space. It is the case that a description of BLS may be expressed in terms of response functions such as those just introduced. In the initial theoretical discussions of BLS from magnetic surfaces[9] and from Damon-Eshbach modes and standing spin waves in films,[10] such a treatment was introduced and employed to obtain quantitative accounts of early spectra. A virtue of this approach is that, as one sees from these papers, the intensity, frequency, and linewidths of the features in the spectra are provided by the theory. While these early papers were directed toward samples with smooth surfaces, if desired the method used in Refs. 9 and 10 is readily adapted to samples with magnetic properties that are modulated in various ways. The response functions described in this paper may be used for this purpose, though as discussed in Sec. I our attention in the present paper is devoted to the FMR response of periodically perturbed films. Because of the possible interest in other applications of the formalism, we present a general discussion and then specialize to the case of FMR absorption.

If defects are present, either in the bulk or on the surfaces, then the response functions $S_{\alpha\beta}(\vec{k}_\parallel,\vec{k}'_\parallel;\Omega)$ will be nonzero when $\vec{k}_\parallel \neq \vec{k}'_\parallel$. If the perturbation is one-dimensionally periodic in real space, say in the form of stripes of some sort with period a_0, then the elements of the response function that are nonzero have $\vec{k}'_\parallel = \vec{k}_\parallel + \vec{g}_m$, where $\vec{g}_m = mg_0\hat{n}$ with $\hat{n}$ a unit vector directed perpendicular to the stripes, $g_0 = 2\pi/a_0$ is the reciprocal lattice vector, and $m = 0, \pm1, \pm2, \ldots$.

The presence of static defects may be described, quite generally, by introducing a perturbation into the Hamiltonian of the form[6]

$$V = \sum_{\vec{k}_\parallel,\vec{k}'_\parallel}\left\{\frac{1}{2}m^\dagger_x(\vec{k}'_\parallel)V_{xx}(\vec{k}'_\parallel,\vec{k}_\parallel)m_x(\vec{k}_\parallel) + m^\dagger_x(\vec{k}'_\parallel)V_{xy}(\vec{k}'_\parallel,\vec{k}_\parallel)m_y(\vec{k}_\parallel) + \frac{1}{2}m^\dagger_y(\vec{k}'_\parallel)V_{yy}(\vec{k}'_\parallel,\vec{k}_\parallel)m_y(\vec{k}_\parallel)\right\}. \tag{3}$$

A discussion of the structure of the matrix elements in Eq. (3) for perturbations on the surface or interface of various sorts can be found in Ref. 6. In the present paper, we shall consider a film upon which stripes are present on the surface. The nature of the matrix elements for this case will be discussed below, with a low-anisotropy material such as Permalloy in mind. For any periodic structure such as that just described, the nonzero matrix elements of $V_{\alpha\beta}(\vec{k}'_\parallel,\vec{k}_\parallel)$ are those for which $\vec{k}'_\parallel = \vec{k}_\parallel + \vec{g}_m$, very much as in the response functions themselves.

We shall proceed for the moment through use of the general form of the perturbation as given in Eq. (3). The response functions $S_{\alpha\beta}(\vec{k}_\parallel,\vec{k}'_\parallel;\Omega)$ may be described as the Fourier transform with respect to time of a Kubo response function formed from the operators $\{m_x(\vec{k}_\parallel)\}$. These operators are time dependent, in the Heisenberg representation. The explicit form of the Kubo formulas are given in Eq. (27) of Ref. 6. One proceeds by generating the equations of motion for these objects, as discussed earlier.[6] For this one needs

to supplement Eq. (3) by the Hamiltonian of the perfect, unperturbed film:

$$E_0 = \frac{1}{2M_S}\sum_{\vec{k}_\parallel}\{H_x(\vec{k}_\parallel)m_x^\dagger(\vec{k}_\parallel)m_x(\vec{k}_\parallel) + H_y(\vec{k}_\parallel)m_y^\dagger(\vec{k}_\parallel)m_y(\vec{k}_\parallel)\}. \quad (4)$$

After the equations of motion are generated, damping is added in a phenomenological manner, using the LLG equation as a guide. After some algebra, which uses constraints on the matrix elements in Eq. (3) from the requirement that this form must be Hermitian, one may arrange the equations of motion to become integral equations in wave vector space. These read

$$S_{xx}(\vec{k}_\parallel, \vec{k}'_\parallel;\Omega) = \tilde{S}^0_{xx}(\vec{k}_\parallel;\Omega)\delta_{\vec{k}_\parallel,\vec{k}'_\parallel} - \sum_{\alpha=x,y}\sum_{\vec{k}''_\parallel}\tilde{S}^0_{x\alpha}(\vec{k}_\parallel;\Omega)V^*_{x\alpha}(\vec{k}''_\parallel, \vec{k}_\parallel)S_{xx}(\vec{k}''_\parallel, \vec{k}'_\parallel;\Omega) - \sum_{\alpha=x,y}\sum_{\vec{k}''_\parallel}\tilde{S}^0_{x\alpha}(\vec{k}_\parallel;\Omega)V_{\alpha y}(\vec{k}_\parallel, \vec{k}''_\parallel)S_{yx}(\vec{k}''_\parallel, \vec{k}'_\parallel;\Omega), \quad (5a)$$

$$S_{yx}(\vec{k}_\parallel, \vec{k}'_\parallel;\Omega) = \tilde{S}^0_{yx}(\vec{k}_\parallel;\Omega)\delta_{\vec{k}_\parallel,\vec{k}'_\parallel} - \sum_{\alpha=x,y}\sum_{\vec{k}''_\parallel}\tilde{S}^0_{y\alpha}(\vec{k}_\parallel;\Omega)V^*_{x\alpha}(\vec{k}''_\parallel, \vec{k}_\parallel)S_{xx}(\vec{k}''_\parallel, \vec{k}'_\parallel;\Omega) - \sum_{\alpha=x,y}\sum_{\vec{k}''_\parallel}\tilde{S}^0_{y\alpha}(\vec{k}_\parallel;\Omega)V_{\alpha y}(\vec{k}_\parallel, \vec{k}''_\parallel)S_{yx}(\vec{k}''_\parallel, \vec{k}'_\parallel;\Omega). \quad (5b)$$

A similar set of equations has been derived for the response functions S_{xy} and S_{yy}, and can be found in the Appendix. The four equations that describe our four sets of response functions break down into a set of two equations in which S_{xx} and S_{yx} are coupled, and into a set of two in which S_{xy} and S_{yy} are coupled. In what follows, we focus on the first set.

For reasons that will be clear shortly, we wish to iterate Eq. (5a) and Eq. (5b) so that the terms on the right-hand side are second order in the perturbation matrix elements $V_{\alpha\beta}(\vec{k}_\parallel, \vec{k}'_\parallel)$. We assume as we do this that the diagonal elements in the wave vector, $V_{\alpha\beta}(\vec{k}_\parallel, \vec{k}_\parallel)$, are zero. If, for some choice of a defect structure one wishes to analyze the diagonal matrix elements are nonzero, they can be adsorbed into the unperturbed Hamiltonian E_0 and the discussion is then phrased in terms of spin waves renormalized by the diagonal terms. Notice that the diagonal elements of V_{xx} and V_{yy} can be absorbed by simply incorporating them into the fields $H_{x,y}(\vec{k}_\parallel)$. A nonzero value for $V_{xy}(\vec{k}_\parallel, \vec{k}_\parallel)$ will, after inclusion into E_0, alter the ellipticity of the zero-order modes slightly. One may diagonalize the Hamiltonian if this term is present and rewrite the theory in terms of the new amplitudes. For the example explored here, $V_{xy}(\vec{k}_\parallel, \vec{k}'_\parallel)$ vanishes identically so this issue does not arise.

When Eq. (5a) and Eq. (5b) are iterated as just discussed, one finds

$$S_{xx}(\vec{k}_\parallel, \vec{k}'_\parallel;\Omega) = \tilde{S}^0_{xx}(\vec{k}_\parallel;\Omega)\delta_{\vec{k}_\parallel,\vec{k}'_\parallel} + \sum_{\alpha,\beta=x,y}\sum_{\vec{k}''_\parallel}\tilde{S}^0_{x\alpha}(\vec{k}_\parallel;\Omega) \times \Sigma_{\alpha\beta}(\vec{k}_\parallel, \vec{k}''_\parallel;\Omega)S_{\beta x}(\vec{k}''_\parallel, \vec{k}'_\parallel;\Omega), \quad (6a)$$

$$S_{yx}(\vec{k}_\parallel, \vec{k}'_\parallel;\Omega) = \tilde{S}^0_{yx}(\vec{k}_\parallel;\Omega)\delta_{\vec{k}_\parallel,\vec{k}'_\parallel} + \sum_{\alpha,\beta=x,y}\sum_{\vec{k}''_\parallel}\tilde{S}^0_{y\alpha}(\vec{k}_\parallel;\Omega) \times \Sigma_{\alpha\beta}(\vec{k}_\parallel, \vec{k}''_\parallel;\Omega)S_{\beta x}(\vec{k}''_\parallel, \vec{k}'_\parallel;\Omega), \quad (6b)$$

where

$$\Sigma_{\alpha x}(\vec{k}_\parallel, \vec{k}'_\parallel;\Omega) = \sum_{\beta=x,y}\sum_{\vec{k}''_\parallel}\big[V^*_{x\alpha}(\vec{k}''_\parallel, \vec{k}_\parallel)\tilde{S}^0_{x\beta}(\vec{k}''_\parallel;\Omega) + V_{\alpha y}(\vec{k}_\parallel, \vec{k}''_\parallel)\tilde{S}^0_{y\beta}(\vec{k}''_\parallel;\Omega)\big]V^*_{x\beta}(\vec{k}'_\parallel, \vec{k}''_\parallel), \quad (7a)$$

$$\Sigma_{\alpha y}(\vec{k}_\parallel, \vec{k}'_\parallel;\Omega) = \sum_{\beta=x,y}\sum_{\vec{k}''_\parallel}\big[V^*_{x\alpha}(\vec{k}''_\parallel, \vec{k}_\parallel)\tilde{S}^0_{x\beta}(\vec{k}''_\parallel;\Omega) + V_{\alpha y}(\vec{k}_\parallel, \vec{k}''_\parallel)\tilde{S}^0_{y\beta}(\vec{k}''_\parallel;\Omega)\big]V_{\beta y}(\vec{k}''_\parallel, \vec{k}'_\parallel). \quad (7b)$$

We comment on the structure of Eqs. (6) and Eqs. (7). First, in the language of many-body theory, the set of objects $\tilde{S}^0_{\alpha\beta}$ are the Green's functions for spin waves in the perfect, unperturbed film. These have matrix form, by virtue of the elliptical character of spin wave precession in the thin film. Then the four functions $S_{\alpha\beta}$ are the Green's functions for the spin waves of the disordered film. They are nondiagonal in wave vector $\vec{k}_\parallel$ because in the presence of disorder, the wave vector is no longer a "good quantum number"; the normal modes no longer are simple plane waves. Equations (6) and (7) are, for the general class of problems described by our formalism, the spin wave equivalent of the well-known Dyson equation of many-body physics. The matrix $\Sigma_{\alpha\beta}$ is the proper self-energy of the spin waves, and this matrix contains information on both disorder-induced frequency shifts of the modes and their lifetimes. As noted above, this formalism was employed earlier to describe the two-magnon contribution to the FMR linewidth and also the frequency shift of the FMR mode from two-magnon coupling.[6,7] For these discussions, the disorder responsible for the two-magnon interactions had a random character.

In the present paper, we are interested in applying the formalism to describe the interaction of spin waves with a periodic defect structure of one-dimensional character. Then for a given choice of $\vec{k}_\parallel$, the only nonzero matrix elements of $S_{\alpha\beta}(\vec{k}_\parallel, \vec{k}'_\parallel;\Omega)$ are those with $\vec{k}'_\parallel = \vec{k}_\parallel + \vec{g}_m$ where, if a_0 is the length of the unit cell of the structure (see Fig. 1), $g_0 = 2\pi/a_0$ and $\hat{n}$ is a unit vector in the direction of the periodicity.

For the one-dimensional periodic structure just described, for a given choice of $\vec{k}'_\parallel$, Eqs. (6) reduce to two coupled equations for the set of propagators $S^{(m)}_{\alpha\beta}(\vec{k}_\parallel, \vec{k}'_\parallel;\Omega) = S_{\alpha\beta}(\vec{k}_\parallel, \vec{k}_\parallel + \vec{g}_m;\Omega)$. For any desired picture of the perturbation, one can develop a description of the nonzero matrix elements in Eq. (3) and proceed to solve Eqs. (6) numerically by an appropriate truncation of the set of equations and then using a matrix inversion.

If the periodic perturbation is modest in strength, then from Eqs. (6) one may develop a spin wave analog of the Brillouin-Wigner perturbation theory of quantum mechanics. We shall proceed in this manner. We will then be able to obtain simple analytical expressions for the response functions that provide insight into the influence of the periodic perturbation. These forms are easily employed to do explicit calculations.

Consider Eq. (6a) for the diagonal component of the propagator $S_{xx}(\vec{k}_\parallel, \vec{k}_\parallel; \Omega)$ and write this in the form

$$\begin{aligned} &S_{xx}(\vec{k}_\parallel, \vec{k}_\parallel; \Omega) \\ &\quad = \tilde{S}^0_{xx}(\vec{k}_\parallel; \Omega) + \sum_{\alpha,\beta=x,y} \tilde{S}^0_{x\alpha}(\vec{k}_\parallel; \Omega)\Sigma_{\alpha\beta}(\vec{k}_\parallel, \vec{k}_\parallel; \Omega)S_{\beta x}(\vec{k}_\parallel, \vec{k}_\parallel; \Omega) \\ &\qquad + \sum_{\alpha,\beta=x,y}\sum_{m\neq 0} \tilde{S}^0_{x\alpha}(\vec{k}_\parallel; \Omega)\Sigma_{\alpha\beta}(\vec{k}_\parallel, \vec{k}_\parallel + \vec{g}_m; \Omega) \\ &\qquad \times S_{\beta x}(\vec{k}_\parallel + \vec{g}_m, \vec{k}_\parallel; \Omega). \end{aligned} \tag{8}$$

The off-diagonal element in wave vector of $S_{\beta x}$ in the third term on the right side of Eq. (8) is nonzero only by virtue of the perturbation. In a perturbation theoretic expansion, each contribution in each order of iteration is always one order higher than the contribution from the second term on the right-hand side of Eq. (8). We thus set the third term on the right-hand side of Eq. (8) aside, and we proceed in a similar manner in our treatment of Eq. (6b). This procedure is equivalent to summing "dominant diagrams" in various other forms of self-consistent perturbation theory. When we do this, we then have a set of two simple algebraic equations for $S_{xx}(\vec{k}_\parallel, \vec{k}_\parallel; \Omega)$ and $S_{yx}(\vec{k}_\parallel, \vec{k}_\parallel; \Omega)$. These have the form

$$\begin{aligned} S_{xx}(\vec{k}_\parallel, \vec{k}_\parallel; \Omega) &= \tilde{S}^0_{xx}(\vec{k}_\parallel; \Omega) + \sum_{\alpha,\beta=x,y} \tilde{S}^0_{x\alpha}(\vec{k}_\parallel; \Omega) \\ &\quad \times \Sigma_{\alpha\beta}(\vec{k}_\parallel, \vec{k}_\parallel; \Omega)S_{\beta x}(\vec{k}_\parallel, \vec{k}_\parallel; \Omega), \end{aligned} \tag{9a}$$

$$\begin{aligned} S_{yx}(\vec{k}_\parallel, \vec{k}_\parallel; \Omega) &= \tilde{S}^0_{yx}(\vec{k}_\parallel; \Omega) + \sum_{\alpha,\beta=x,y} \tilde{S}^0_{y\alpha}(\vec{k}_\parallel; \Omega) \\ &\quad \times \Sigma_{\alpha\beta}(\vec{k}_\parallel, \vec{k}_\parallel; \Omega)S_{\beta x}(\vec{k}_\parallel, \vec{k}_\parallel; \Omega). \end{aligned} \tag{9b}$$

If the off-diagonal matrix elements in the wave vector of the response functions are desired, then one can proceed by inserting the solution of Eqs. (9) into the right-hand side of Eqs. (5). We then have

$$\begin{aligned} &S_{xx}(\vec{k}_\parallel + \vec{g}_m, \vec{k}_\parallel; \Omega) \\ &\quad = -\sum_{\alpha=x,y} \tilde{S}^0_{x\alpha}(\vec{k}_\parallel + \vec{g}_m; \Omega)V^*_{x\alpha}(\vec{k}_\parallel, \vec{k}_\parallel + \vec{g}_m)S_{xx}(\vec{k}_\parallel, \vec{k}_\parallel; \Omega) \\ &\qquad - \sum_{\alpha=x,y} \tilde{S}^0_{x\alpha}(\vec{k}_\parallel + \vec{g}_m; \Omega)V_{\alpha y}(\vec{k}_\parallel + \vec{g}_m, \vec{k}_\parallel)S_{yx}(\vec{k}_\parallel, \vec{k}_\parallel; \Omega), \end{aligned} \tag{10a}$$

$$\begin{aligned} &S_{yx}(\vec{k}_\parallel + \vec{g}_m, \vec{k}_\parallel; \Omega) \\ &\quad = -\sum_{\alpha=x,y} \tilde{S}^0_{y\alpha}(\vec{k}_\parallel + \vec{g}_m; \Omega)V_{x\alpha}(\vec{k}_\parallel + \vec{g}_m, \vec{k}_\parallel)S_{xx}(\vec{k}_\parallel, \vec{k}_\parallel; \Omega) \\ &\qquad - \sum_{\alpha=x,y} \tilde{S}^0_{y\alpha}(\vec{k}_\parallel + \vec{g}_m; \Omega)V_{\alpha y}(\vec{k}_\parallel + \vec{g}_m, \vec{k}_\parallel)S_{yx}(\vec{k}_\parallel, \vec{k}_\parallel; \Omega). \end{aligned} \tag{10b}$$

On the right-hand side of Eqs. (10), one is to insert the expressions for $S_{\alpha x}(\vec{k}_\parallel, \vec{k}_\parallel; \Omega)$ that emerge from the solution of the two algebraic equations stated in Eqs. (5).

If the film is exposed to radiation polarized parallel to the x axis, which lies in the plane perpendicular to the magnetization (see Fig. 1), then the energy absorption rate is proportional to $\Omega\mathrm{Im}\{S_{xx}\}$. In what follows, we shall focus our attention on $S_{xx}(\vec{k}_\parallel, \vec{k}_\parallel; \Omega)$. The solutions of Eqs. (9) have the form, with reference to wave vector and frequency suppressed,

$$\begin{aligned} S_{xx} &= \left\{ \tilde{S}^0_{xx}\left(1 - \sum_\alpha \tilde{S}^0_{y\alpha}\Sigma_{\alpha y}\right) + \tilde{S}^0_{yx}\left(\sum_\alpha \tilde{S}^0_{x\alpha}\Sigma_{\alpha y}\right)\right\} \Big/ \\ &\quad \times \left\{ \left(1 - \sum_\alpha \tilde{S}^0_{x\alpha}\Sigma_{\alpha x}\right)\left(1 - \sum_\alpha \tilde{S}^0_{y\alpha}\Sigma_{\alpha y}\right) \right. \\ &\quad \left. - \left(\sum_\alpha \tilde{S}^0_{x\alpha}\Sigma_{\alpha y}\right)\left(\sum_\alpha \tilde{S}^0_{y\alpha}\Sigma_{\alpha x}\right)\right\}. \end{aligned} \tag{11}$$

In the limit of weak perturbations, one may ignore the corrections to the numerator with origin in the perturbation matrix elements, and in the denominator one may retain only terms that are quadratic in the matrix elements. This leaves us with the simple form

$$S_{xx} \approx \frac{\tilde{S}^0_{xx}}{1 - \sum_{\alpha,\beta} \tilde{S}^0_{\alpha\beta}\Sigma_{\beta\alpha}}. \tag{12}$$

This concludes our discussion of the formalism. The numerical calculations we present below will be based on the use of Eq. (12). To proceed further, one needs a specific picture of the periodic defect structure along with the interactions that dominate the matrix elements that enter Eq. (3).

B. Matrix elements for a model film

We wish to present a series of numerical studies we have carried out based on Eq. (12). To proceed, we require a particular model of the nature of the periodic defects. Of interest to us are recent experiments by Barsukov and colleagues,[5] who have explored the FMR response of Permalloy films in which the magnetization in a thin layer on the outer surface is modulated periodically. The samples were fabricated by a lithographic procedure in which Cr was injected into the Permalloy film in such a way as to modulate the magnetization of the film in a stripelike manner near one surface. It is difficult to model such samples in a fully quantitative way, since the magnetization within the Cr-doped regions and its profile in both the direction normal to the surface and that parallel to it are not well known. Also there are other issues, such as the influence on the Permalloy of the residual Cr layer that remains after the sample preparation process is complete. Thus, we shall proceed to explore the structure illustrated in Fig. 1, wherein stripes are present on the surface of a film. The material in the stripes is the same as that in the main body of the film, in our picture. It is possible to find explicit expressions for the matrix elements in Eq. (3) from this model, as we shall see below. The principal features in the FMR spectrum produced by such a model system can be expected to be quite appropriate to the samples utilized in Ref. 5, though a fully quantitative account of the data would require more information on the magnetization profile in the perturbed regions of the actual samples.

We note that in an earlier theoretical study, detailed calculations were presented of the spatial variation of the magnetization in a film whose surfaces were modulated in a stepwise fashion.[11] We use the results of this paper to describe the stray dipole fields generated from the array of

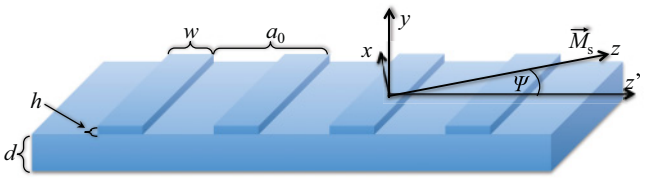

FIG. 1. (Color online) The model film explored in the present paper. The z' axis is perpendicular to the steps on the surface, and the magnetization is parallel to the z axis and makes an angle Ψ with respect to the steps. The dimensions of the various structures are illustrated, and for reasons discussed in the text the magnetization is assumed spatially uniform everywhere.

stripes illustrated in Fig. 1. In a low-anisotropy material such as Permalloy, such stray fields will be responsible for the perturbation term in Eq. (3). The presence of the steps will also induce anisotropy which will want to orient the magnetization parallel to the stripes, as also discussed in Ref. 11. However, in the experiments of interest to us, the applied Zeeman field is large compared to this anisotropy field and we ignore its influence in the interests of simplicity. It is our understanding that the step-induced anisotropy field is not evident in its effect in the experiments.[5]

The interaction between the magnetization and the stray dipolar fields has the form

$$V = -\frac{1}{2}\int d^3r\, H_z^{\rm step}(\vec{r})M_z(\vec{r}) - \frac{1}{2}\int d^3r\left\{H_x^{\rm step}(\vec{r})m_x(\vec{r}) + H_y^{\rm step}(\vec{r})m_y(\vec{r})\right\}, \quad (13)$$

where $\vec{H}^{\rm step}(\vec{r})$ is the static field generated by the magnetic poles on the step faces and also by modulation of the magnetization in the film by the steps. We shall see that the latter effect is very important. The last two terms in Eq. (13) are linear in the transverse magnetization. It is these terms that lead to canting of the magnetization away from the spatially uniform magnetization characteristic of the perfect film, as discussed in Ref. 11. These terms are incorporated into the description of the modulation of the magnetization direction in the ground state and do not play a role here. The term of interest presently is the first term, and with $M_z(\vec{r}) \simeq M_S - (1/2M_S)\{m_x^2(\vec{r}) + m_y^2(\vec{r})\}$ we have

$$V = \frac{1}{4M_S}\int d^3r\, H_z^{\rm step}(\vec{r})\left\{m_x^2(\vec{r}) + m_y^2(\vec{r})\right\}. \quad (14)$$

From Eq. (14), it is evident that in Eq. (3), $V_{xy} = 0$ and $V_{xx} = V_{yy}$ for this picture. The stray field $\vec{H}^{\rm step}(\vec{r})$ may be written as $-\vec{\nabla}\Phi_M^{\rm step}(\vec{r})$, where $\Phi_M^{\rm step}(\vec{r})$ is a magnetic potential.

Here we will confine our attention to the case where the magnetization is perpendicular to the stripes, so that the angle Ψ in Fig. 1 vanishes. In the limit the film is thick compared to the exchange length, the magnetic potential is well approximated by the form appropriate to a semi-infinite medium with stripes such as those illustrated in Fig. 1 on its surface. The magnetic potential can, in this limit, be described by the elementary form in Eq. (45) of Ref. 11. For this purpose, we need to describe $\xi^>(z)$, the height of the actual surface above the nominal film surface in a Fourier series. For the geometry in Fig. 1 we have

$$\xi^>(z) = \pi h\sum_{m=-\infty}^{\infty}\frac{\sin[m\pi w/a_0]}{m}e^{img_0z}. \quad (15)$$

It is assumed that the origin of the coordinate system lies at the center of a stripe. Then for the z component of the stray field, one finds within the film where $y < d$[12]

$$H_z^{\rm step}(y,z) = -4M_Sg_0h\sum_{m=1}^{\infty}\sin\left[\frac{m\pi w}{a_0}\right]\cos[mg_0z]\lambda(mg_0) \times\{b_0(mg_0)e^{-\alpha_0(mg_0)|d-y|} - b_x(mg_0)e^{-\alpha_x(mg_0)|d-y|}\}. \quad (16)$$

On the right-hand side of Eq. (16), $\lambda(Q) = 2\alpha_0(Q)\alpha_x(Q)/\{[\alpha_x(Q) - \alpha_0(Q)][\alpha_x(Q) + \alpha_0(Q) - |Q|]\}$, $b_{0,x}(Q) = [\alpha_{x,0}(Q) - |Q|][\alpha_{0,x}(Q) + |Q|]$, and finally, in the notation used in the present paper,

$$\alpha_{\substack{0\\x}}(Q) = \sqrt{Q^2 + \frac{B_0}{2D}\left[1 \mp \sqrt{1 + \frac{16\pi M_S}{B_0^2}DQ^2}\right]}. \quad (17)$$

An interesting limit to consider is the limit in which the exchange stiffness $D \to \infty$. One finds that $\alpha_0(Q) \to Q - (\pi M_S/D)^{1/2} + \cdots$ and $\alpha_x(Q) \to Q + (\pi M_S/D)^{1/2} + \cdots$ in this limit. Thus $b_0(Q)e^{-\alpha_0(Q)|d-y|} - b_x(Q)e^{-\alpha_x(Q)|d-y|} \to \{[\alpha_x(Q) - \alpha_0(0)]/2Q\}e^{-mg_0|d-y|}$ so that as $D \to \infty$ one finds

$$H_z^{\rm step}(y,z) \to H_z^{\infty}(y,z) = -4M_Sg_0h \times\sum_{m=1}^{\infty}\sin\left[\frac{m\pi w}{a_0}\right]\cos[mg_0z]e^{-mg_0|d-y|}. \quad (18)$$

The expression in Eq. (18) is the stray field one would calculate on the basis of a picture in which the magnetization in the sample is spatially uniform everywhere, with direction unaffected by the presence of the steps. The field is then produced by an effective magnetic charge per unit area of magnitude M_S on the faces of the steps which alternates in sign as one moves down the line perpendicular to the steps.

We are in a very different limit than that of large D, for samples such as those studied in Ref. 5. To illustrate this, we consider a special limit of Eq. (16). The length scale in a material with zero anisotropy is set by the width of a Neel wall, which is $L_N = (D/8\pi M_S)^{1/2}$. In wave vector space, the scale is thus set by $Q_N = 2\pi/L_N = 4\pi(2\pi M_S/D)^{1/2} \sim 10^7\ {\rm cm}^{-1}$. The domain wall thickness is roughly 100 Å, or 10 nm in Permalloy. Suppose we are interested in length scales long compared to L_N and consequently wave vectors $Q = mg_0$ that are small compared to Q_N. For parameters of interest to us, one finds $\alpha_x \approx 50\alpha_0$, so the second term on the right-hand side of Eq. (16) can be neglected. Also in this limit, $\alpha_0(Q) \approx Q(H_0/B_0)^{1/2}$ is sufficiently small that the stray field is spatially uniform across the film, as is its high-field form in Eq. (18). When limiting forms of the various quantities that

enter Eq. (16) are introduced, we find that for the spatial Fourier components of interest to us, to very good approximation we may write

$$H_z^{\rm step}(y,z) \approx r H_z^{\infty}(y,z), \tag{19}$$

where $r = 2H_0^{1/2}[B_0^{1/2} + H_0^{1/2}]$.

We see from Eq. (19) that for low applied magnetic fields the Fourier components of the stray fields are reduced greatly in strength, for small wave vectors by step-induced modulations of the ground-state magnetization. The "rigid magnetization" picture very substantially overestimates the Fourier components of the stray fields of interest to the present discussion. As the applied field increases, when H_0 becomes much larger than $4\pi M_S$ the Fourier components of the stray field evolve into the rigid magnetization result. The behavior of the Fourier components of the stray field with $Q \ll Q_N$ is controlled only by dipolar interactions and exchange does not enter their description.

From Eq. (16) it is straightforward to calculate the matrix element V_{xx}. One finds

$$V_{xx}(\vec{k}'_\parallel, \vec{k}_\parallel) = -g_0 h \sum_{m=1}^{\infty} \sin\left[\frac{m\pi w}{a_0}\right] \lambda(mg_0)\eta(mg_0) \times \left\{\delta_{\vec{k}'_\parallel, \vec{k}_\parallel + \vec{g}_m} + \delta_{\vec{k}'_\parallel, \vec{k}_\parallel - \vec{g}_m}\right\}, \tag{20}$$

where $\lambda(Q)$ is defined below Eq. (16) and $\eta(Q)$ is given by

$$\eta(Q) = b_0(Q)\frac{1 - e^{-\alpha_0(Q)d}}{\alpha_0(Q)d} - b_x(Q)\frac{1 - e^{-\alpha_x(Q)d}}{\alpha_x(Q)d}. \tag{21}$$

Recall that $V_{xx} = V_{yy}$ and $V_{xy} = 0$.

C. Film response in ferromagnetic resonance

In what follows, our interest will center on the function $S_{xx}(\vec{k}'_\parallel, \vec{k}_\parallel; \Omega)$ evaluated for the case where $\vec{k}_\parallel = \vec{k}'_\parallel = 0$. This describes the component of the total dynamic moment parallel to the surface induced by a spatially uniform microwave field polarized parallel to the surface. The imaginary part of this function describes the FMR absorption spectrum of the film. In what follows, we shall refer to this function as $\bar{S}_{xx}(\Omega)$. Equation (12) in combination with the matrix element given in Eq. (20) leads to

$$\bar{S}_{xx}(\Omega) = \frac{\gamma^2 M_S \tilde{H}_y(0)}{\tilde{\Omega}^2_{\rm FMR} - \Omega^2 - \Gamma(\Omega)}, \tag{22}$$

where $\tilde{\Omega}^2_{\rm FMR} = \gamma^2 \tilde{H}_x(0)\tilde{H}_y(0)$ and

$$\Gamma(\Omega) = 2g_0^2 h^2 (\gamma M_S)^2 \left[\gamma^2\left\{\tilde{H}_x^2(0) + \tilde{H}_y^2(0)\right\} + 2\Omega^2\right] \times \sum_{m=1}^{\infty} \frac{\{\sin[m\pi w/a_0]\lambda(mg_0)\eta(mg_0)\}^2}{\tilde{\Omega}(mg_0\hat{z})^2 - \Omega^2}. \tag{23}$$

The intrinsic damping, as described by the factor $i\alpha\Omega$ in the quantities $\tilde{H}_{x,y}(\vec{k}_\parallel) = H_{x,y}(\vec{k}_\parallel) - i\alpha\Omega/\gamma$, is small, so we can simplify the form in Eq. (23) by retaining the influence of this term to lowest order. If we then introduce $\Lambda(\vec{k}_\parallel) = \alpha\Omega\gamma[H_x(\vec{k}_\parallel) + H_y(\vec{k}_\parallel)]$ we have for the real part $\bar{S}^R_{xx}(\Omega)$ and the imaginary part $\bar{S}^I_{xx}(\Omega)$ of the response functions forms that may be written

$$\bar{S}^R_{xx} = \frac{\gamma^2 M_S H_y(0)\left\{\Omega^2_{\rm FMR} - \Omega^2 - \Gamma^R\right\}}{\left\{\Omega^2_{\rm FMR} - \Omega^2 - \Gamma^R\right\}^2 + \{\Lambda(0) + \Gamma^I\}^2}, \tag{24a}$$

$$\bar{S}^I_{xx} = \gamma M_S \frac{\gamma H_y(0)\{\Lambda(0) + \Gamma^I\} - \alpha\Omega\left\{\Omega^2_{\rm FMR} - \Omega^2 - \Gamma^R\right\}}{\left\{\Omega^2_{\rm FMR} - \Omega^2 - \Gamma^R\right\}^2 + \{\Lambda(0) + \Gamma^I\}^2}. \tag{24b}$$

The function $\Gamma^I = \Gamma^I(\Omega)$, which corresponds to the imaginary part of Eq. (23), contains information on the frequency-dependent contribution to the FMR linewidth from the presence of the surface steps. In Sec. III we shall see that this function introduces dramatic structure into the linewidth when the steps are present, when for a range of frequencies, the field is swept in an experiment. The explicit form of this function is

$$\Gamma^I = 2g_0^2 h^2 (\gamma M_S)^2 \sum_{m=1}^{\infty} \frac{\{\sin[m\pi w/a_0]\lambda(mg_0)\eta(mg_0)\}^2}{\{\Omega(mg_0\hat{z})^2 - \Omega^2\}^2 + \Lambda(mg_0\hat{z})^2} \times \{[\gamma^2(H_x(0)^2 + H_y(0)^2) + 2\Omega^2]\Lambda(mg_0\hat{z}) - 2[\Omega(mg_0\hat{z})^2 - \Omega^2]\Lambda(0)\}, \tag{25}$$

while the real part of Eq. (23), $\Gamma^R = \Gamma^R(\Omega)$ which contain information about the step-induced frequency shift of the resonance, is given by

$$\Gamma^R = 2g_0^2 h^2 (\gamma M_S)^2 \sum_{m=1}^{\infty} \frac{\{\sin[m\pi w/a_0]\lambda(mg_0)\eta(mg_0)\}^2}{\{\Omega(mg_0\hat{z})^2 - \Omega^2\}^2 + \Lambda(mg_0\hat{z})^2} \times \{[\gamma^2(H_x(0)^2 + H_y(0)^2) + 2\Omega^2][\Omega(mg_0\hat{z})^2 - \Omega^2] + 2\Lambda(0)\Lambda(mg_0\hat{z})\}. \tag{26}$$

It can be shown that for the samples of interest to us,[5] the frequency shift is negligible. Finally, the FMR linewidth in an experiment where field is swept at fixed frequency, in the presence of the surface steps with magnetization in plane, is given by

$$\Delta B_{\rm FMR} = \frac{\Lambda(0) + \Gamma^I(\Omega_{\rm FMR})}{\gamma^2[H_x(0) + H_y(0)]}. \tag{27}$$

We now turn out attention to numerical calculations based on the expressions displayed in this section.

III. STUDIES OF THE INFLUENCE OF STRIPES ON THE FMR RESPONSE OF THIN FILMS

In this section, we present a series of numerical studies that elucidate the influence of the stripes illustrated in Fig. 1 on the FMR response of a thin Permalloy film. We choose parameters with the samples explored in Ref. 5 in mind. For $4\pi M_S$, appropriate to Permalloy, we use 10 000 G, the gyromagnetic ratio is 2.95 GHz/kG, the exchange stiffness $D = 1.85 \times 10^5$ G×nm^2, and the film thickness d is taken to be 30 nm.[5] From the linewidth data, a value for the LLG damping parameter $\alpha = 0.01$ seems appropriate. The periodicity length a_0 is 250 nm, and the width w in Fig. 1 will be discussed below. For simplicity, in all the numerical calculations the angle between the magnetization and the

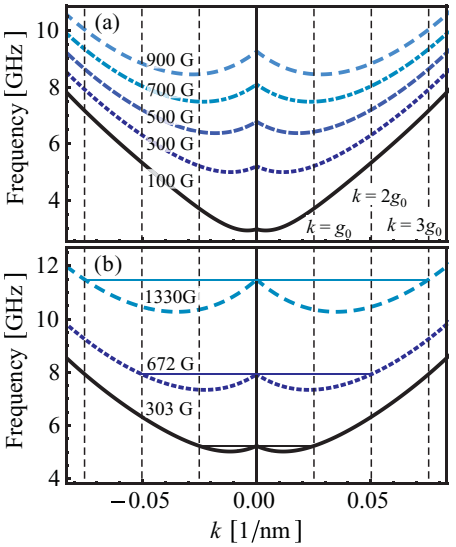

FIG. 2. (Color online) In (a) we show the dispersion relation of spin waves in the perfect film, for a range of applied magnetic fields. The direction of propagation is parallel to the magnetization, and perpendicular to the stripes on the surface of the perturbed film. The vertical dashed lines are Brillouin zone boundaries for the film with stripes. (b) For selected values of the applied magnetic field we have modes with wave vector mg_0, with m an integer, that are degenerate with the zero wave vector FMR mode. For three choices of applied field, we illustrate the dispersion relation when such a degeneracy occurs.

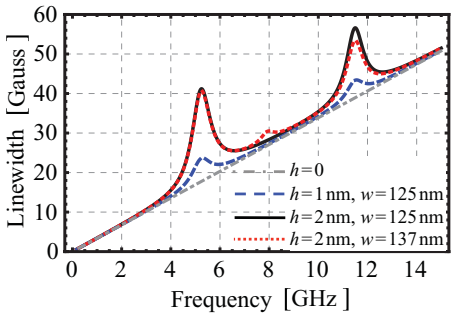

FIG. 3. (Color online) The frequency dependence of the FMR linewidth, as described by Eq. (27). The dot-dashed line is the linewidth for the perfect film. The dotted and full curves are calculated for $h = 2$ nm, while the dashed curve is calculated for $h = 1$ nm. For the full and dashed curves, we have $w = 125$ nm, while $w = 137$ nm for the dotted curve.

perpendicular to the stripes is set to $\Psi = 0$, since our main findings [see Eqs. (23), (25), and (26)] will be proportional to $[\cos(\Psi)]^4$, which means that the features we observe in the linewidth vanish if the magnetization is parallel to the stripes ($\Psi = \pi/2$), and the effect has its maximum strength in the case $\Psi = 0$, as we consider here and as was observed in the experiment of Barsukov and colleagues.[5]

In Fig. 2(a), we show the spin wave dispersion relation in the extended Brillouin zone, for the perfect, unperturbed film for several applied fields. The direction of propagation is parallel to the magnetization, where the dipolar interaction between the spins leads initially to a negative slope in the dispersion relation save for very small applied fields. With increasing wave vector, exchange dominates the dipolar contribution to produce the well-known minimum in the dispersion relation. In the figure we show the position of the Brillouin zone boundaries of interest to our discussion. For special choices of the applied magnetic field, we have spin waves at wave vectors mg_0 that are degenerate with the FMR mode. We illustrate the dispersion curve for three such choices of field in Fig. 2(b). The periodic perturbation couples the FMR mode to these finite wave vector modes in a resonant manner at these special values of the applied magnetic field. This coupling will be responsible for effects in the FMR spectrum discussed below.

In Fig. 3, we show calculations of the frequency dependence of the field linewidth, from Eq. (27). The dotted and full curves are both calculations with the choice $h = 2$ nm. We see prominent structures near 5 GHz and a bit below 12 GHz in both the dotted and full curves. Two features in the linewidth data discussed in Ref. 5 for the sample with $a_0 = 250$ nm are quite close to these frequencies. The dashed curve is a calculation with $h = 1$ nm. We again see two structures at these frequencies, but now the height of the attenuation peaks is much smaller than realized when $h = 2$ nm. It is clear that the origin of these two prominent peaks lies in the degeneracies illustrated in Fig. 2(b). The periodic potential couples the zero wave vector FMR mode to the degenerate spin waves at the wave vectors g_0 and $3g_0$, respectively. Thus, when the FMR mode is excited, energy is transferred to these two modes, and there is highly efficient resonant transfer when the degeneracy condition is satisfied. This provides a new relaxation channel; the energy transferred to the degenerate mode is dissipated by virtue of the damping present in the LLG equation. The full and dashed curves show no feature near 8 GHz, where one realizes degeneracy with the spin wave mode with the wave vector $2g_0$. The reason for this is that the ratio $w/a_0 = 1/2$ in this calculation, so the argument of the factor of $\sin[m\pi w/a_0]$ in Eq. (23) vanishes. Thus the matrix element that couples the FMR mode to the $2g_0$ spin wave vanishes for this choice of w and there is thus no linewidth peak near 8 GHz. The ratio w/a_0 is very close to $1/2$ in the sample,[13] so this attenuation peak is not seen in the data. The dotted curve is calculated for $w = 137$ nm, and we see a modest peak near 8 GHz.

It is difficult for our theory to make quantitative connection with the data in Ref. 5, since the character of the samples used is complex. While the Cr ions penetrate as deeply as 7 nm, a depth far larger than the step heights used in Fig. 3, it is the case as well that the average magnetization in the Cr-doped regions is estimated to be lower than that of the undoped regions by only about 20%,[13] whereas in our model the contrast between the magnetization in the steps and the open areas between the steps is 100%. We also suggest that the variation of the Cr concentration along the x direction in our Fig. 1 is not a simple sharp step in the samples as assumed in our model. In the data on the sample with $a_0 = 250$ nm, the height of the peak near 12 GHz relative to the background is quite similar to that displayed in the dotted and full curves in our Fig. 3, but the experimental peak near 5 GHz is more modest in height than that in theory. The ratio of these two peak heights is clearly controlled by the ratio $R = [V_{xx}(g_0,0)/V_{xx}(3g_0,0)]^2$, and our model with its sharp discontinuity in magnetization, independent of z, overestimates this ratio by perhaps a factor

of two to judge from the size of the low-frequency peak in the blue curve. Without a great deal of information on the spatial distribution of the implanted Cr ions in the samples used in Ref. 5, it is difficult to make a fully quantitative comparison with the data.

As remarked above, the absorption rate is proportional to $\mathrm{Im}\{S_{xx}(\Omega)\}$. A plot of this function gives information on the line shape, whereas the expression in Eq. (27) is a measure only of the full width at half maximum. In Fig. 4(a), we show a plot of the profile of the absorption peak for the feature just below 12 GHz, for four choices of h and with $w = 137$ nm. What we see is that the "skirts" of the absorption line removed in frequency from the peak are not affected greatly by the resonant coupling to the $3g_0$ mode, but the maximum is depressed. The dependence of the full width at half maximum (FWHM) on h is close to the same as that given in Fig. 3 for the resonant magnetic field, but the line shape has changed. The factor of $\Gamma^I(\Omega)$ in Eq. (24b) is strongly frequency dependent as one sweeps through the resonance line, as one sees from Eq. (25). The line shape is thus distorted, with the absorption

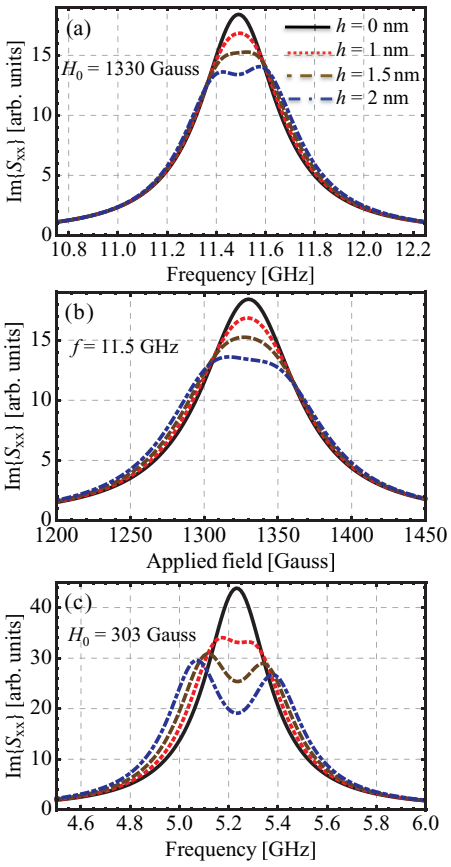

FIG. 4. (Color online) We show plots of the function $\mathrm{Im}\{S_{xx}(\Omega)\}$, which is the absorption line profile, for three cases. In all figures we have $w = 137$ nm, and four values of the step height h are employed: $h = 0$ (solid curve), $h = 1$ nm (dotted curve), $h = 1.5$ nm (dashed curve), and $h = 2$ nm (dot-dashed curve). In (a) we show a frequency sweep of the resonance line in the vicinity of the high-frequency resonance just below 12 GHz, at a fixed field of 1330 G. In (b) we show a field sweep of the same line at fixed frequency (11.5 GHz), and in (c) we show a field sweep of the line near 5 GHz at fixed field (303 G).

in the near vicinity of the peak depressed more strongly than in the wings of the absorption line. In Fig. 4(b), we show $\mathrm{Im}\{S_{xx}(\Omega)\}$ for the case where one does a field rather than a frequency sweep through the resonance. The behavior is rather similar to what one finds for the frequency sweep displayed in Fig. 4(a).

What Fig. 4(a) illustrated is most interesting in our minds. The resonant coupling of the FMR mode to the $3g_0$ spin wave provides an additional channel for energy dissipation, as discussed above. However, it is clear the integrated absorption for the perturbed film is actually *less* than that of the perfectly flat film wherein the additional dissipation channel is not present. What has happened is, near the peak of the absorption line, the additional damping has decreased the amplitude of the spin motion and thus decreased the absorption rate in this spectral regime, in a manner familiar from elementary discussions of damped harmonic oscillators. But as discussed above, the strong frequency variation of $\Gamma^I(\Omega)$ renders this effect absent in the wings, thus returning the absorption rate to its higher value appropriate to the flat film in the wings. The net effect of adding the additional dissipation channel is to *decrease* the integrated absorption. If the added energy dissipation rate were independent of frequency as one sweeps through the resonance, then the wings would be broadened, and the total integrated absorption would increase as expected naively when a new damping channel is added. This effect could be obscured somewhat if the periodic structure were not perfectly periodic, which would have the consequence that the frequency dependence of $\Gamma^I(\Omega)$ would not be as dramatic as described by the theory of the perfect structure. What one would realize in that case is something one might call two-magnon damping, spread out over a certain frequency range whose width would be controlled by the spatial Fourier spectrum of the deviations from perfect periodicity.

In Fig. 4(c), we show a frequency sweep through $\mathrm{Im}\{S_{xx}(\Omega)\}$ for the low-frequency resonance near 5 GHz. Now, for our particular model, we see behavior quite different than that illustrated in Fig. 4(a). For the smallest nonzero value of h employed, we see the depression of the absorption rate near the peak very much as in Fig. 4(a), but then as h increases a splitting of the absorption peak develops. The splitting of the peak has its mathematical origin in the factor of $\Gamma^R(\Omega)$ in Eq. (24b). The periodic perturbation couples the $k_\parallel = 0$ mode to the $k_\parallel = g_0$ mode, and just as in the case of two coupled oscillators there is a frequency splitting. To resolve this splitting in an experiment, the splitting has to be sufficiently large that it can be resolved in the presence of damping. In Fig. 4(a), the role of damping is the primary effect through increasing the FWHM by depressing the absorption at the peak, and in Fig. 4(c) we are in the limit where the coupling is small enough that save for rather small values of h the splitting manifests itself in the spectrum. Evidently such a splitting of the resonance line is not observed in Ref. 5. As we noted above, our model appears to overestimate the strength of the intermode coupling in the 5 GHz region, possibly for reasons such as discussed above.

We thus have a weak-coupling regime and a strong-coupling regime. In the weak-coupling regime, damping is sufficiently strong that the splitting induced by the resonant coupling between the two modes linked by the periodic structure is not

resolved, and the FWHM of the absorption line is increased by the mechanism discussed above. In the strong-coupling regime, the periodic perturbation is sufficiently strong that the splitting is fully resolved as in Fig. 4(c). It is the case that the data reported in Ref. 5 is an example of the weak-coupling limit.

IV. CONCLUDING REMARKS

We have developed a theory of the interaction of spin waves with static, periodic defects in thin ferromagnetic films. The structure of the theory is patterned after Brillouin-Wigner perturbation theory in quantum mechanics, wherein the frequencies or energies of new states emerge from a self-consistent perturbation theoretic structure. Our theory provides the full response functions that describe the response of the film to externally applied microwave fields, and the phenomenological damping as contained in the LLG equation is included fully. The discussion in Sec. III shows that the description of the film response simply in terms of a full width of the resonance line at half maximum does not give a complete picture of the underlying physics.

It is the case, as we have seen, that the FWHM does show a resonant-like response at those special applied fields and frequencies where resonant coupling manifests itself, but the description of the line profile is not fully characterized by such a single measure.

Our discussion suggests further experiments. First, in the weak-coupling regime, of great interest would be detailed studies of the absorption line profiles. It would be very interesting to first measure the absorption line profile for a perfect film, either by a frequency scan via a spectrum analyzer or via a magnetic field sweep. Then this could be repeated for a perturbed film that shows a peak in the apparent linewidth such as that seen in our Fig. 3 and the figures in Ref. 5, and the two spectra superimposed to see whether indeed the "skirts" are similar but the peak absorption decreased, as in our calculations. Then, of course, it would be very interesting to see films prepared with a periodic perturbation strong enough to enter the strong-coupling regime. We note that by lithographic methods, it should be possible to prepare films of the nature illustrated in Fig. 1. Such a structure should be able to be placed in contact with the model calculations discussed here. Indeed, the model set forth here was motivated by conversations about such samples.[14]

Finally we remind the reader that while we have focused our attention on a particular model of a periodic defect structure, that illustrated in Fig. 1, it is the case that the general formalism will apply to a wide class of periodic defect structures. Also, as noted in Sec. I, if desired the general formalism can be applied to the description of Brillouin light scattering from periodically perturbed films. We remark that in computer simulation studies of eigenvectors and eigenfrequencies in periodically perturbed films, damping is usually not included and we see from our examples that it can enter critically in controlling the film response. Also in numerical simulations, no scheme for normalizing the eigenvectors appropriately are included in any of the standard packages, so relative intensities of various lines in Brillouin spectra cannot be addressed in these schemes. Our formalism fully incorporates, implicitly, the appropriate normalization as one sees from well-known general discussions of Green's functions. For instance, as demonstrated many years ago, a response function approach such as described here does an excellent job of describing relative intensities of lines in BLS spectra for ideal films and surfaces.[9,10] New physical information can be extracted from such studies, such as the role of spin pinning both at surfaces and buried interfaces.

ACKNOWLEDGMENTS

We have benefited greatly by stimulating discussions with I. Barsukov, J. Lindner, C. Hassel, M. Farle, and R. Arias. The research of D.L.M. is supported by the US Department of Energy through Grant No. DE-FG03-84ER-45083. P.L. acknowledges support from FONDECYT 1120618 and the "Centro para el Desarrollo de la Ciencia y la Nanotecnología" CEDENNA FB0807.

APPENDIX

The remaining expressions for the response functions in Eqs. (5) can be cast in the form

$$S_{xy}(\vec{k}_\parallel,\vec{k}'_\parallel;\Omega)=\tilde{S}^0_{xy}(\vec{k}_\parallel;\Omega)\delta_{\vec{k}_\parallel,\vec{k}'_\parallel}-\sum_{\alpha=x,y}\sum_{\vec{k}''_\parallel}\tilde{S}^0_{x\alpha}(\vec{k}_\parallel;\Omega)V^*_{x\alpha}(\vec{k}''_\parallel,\vec{k}_\parallel)S_{xy}(\vec{k}''_\parallel,\vec{k}'_\parallel;\Omega)-\sum_{\alpha=x,y}\sum_{\vec{k}''_\parallel}\tilde{S}^0_{x\alpha}(\vec{k}_\parallel;\Omega)V_{\alpha y}(\vec{k}_\parallel,\vec{k}''_\parallel)S_{yy}(\vec{k}''_\parallel,\vec{k}'_\parallel;\Omega) \tag{A1}$$

and

$$S_{yy}(\vec{k}_\parallel,\vec{k}'_\parallel;\Omega)=\tilde{S}^0_{yy}(\vec{k}_\parallel;\Omega)\delta_{\vec{k}_\parallel,\vec{k}'_\parallel}-\sum_{\alpha=x,y}\sum_{\vec{k}''_\parallel}\tilde{S}^0_{y\alpha}(\vec{k}_\parallel;\Omega)V^*_{x\alpha}(\vec{k}''_\parallel,\vec{k}_\parallel)S_{xy}(\vec{k}''_\parallel,\vec{k}'_\parallel;\Omega)-\sum_{\alpha=x,y}\sum_{\vec{k}''_\parallel}\tilde{S}^0_{y\alpha}(\vec{k}_\parallel;\Omega)V_{\alpha y}(\vec{k}_\parallel,\vec{k}''_\parallel)S_{yy}(\vec{k}''_\parallel,\vec{k}'_\parallel;\Omega). \tag{A2}$$

*pedro.landeros@usm.cl

[1] G. Gubbiotti, S. Tacchi, M. Madami, G. Carlotti, A. O. Adeyeye, and M. Kostylev, J. Phys. D: Appl. Phys. **43**, 264003 (2010).

[2] If the spheres are large enough that the single-sphere spin waves may be viewed as purely dipolar; see R. Arias and D. L. Mills, Phys. Rev. B **70**, 104425 (2004). In the nanoscale regime, inclusion of exchange in the single-sphere response is essential. See R. Arias, P. Chu, and D. L. Mills, Phys. Rev. B **71**, 224410 (2005).

[3] R. Arias and D. L. Mills, Phys. Rev. B **67**, 094423 (2003).

[4]J. Topp, D. Heitmann, M. P. Kostylev, and D. Grundler, Phys. Rev. Lett. **104**, 207205 (2010).
[5]I. Barsukov, F. M. Römer, R. Meckenstock, K. Lenz, J. Lindner, S. Hemken to Krax, A. Banholzer, M. Körner, J. Grebing, J. Fassbender, and M. Farle, Phys. Rev. B **84**, 140410(R) (2011).
[6]R. Arias and D. L. Mills, Phys. Rev. B **60**, 7395 (1999).
[7]P. Landeros, R. E. Arias, and D. L. Mills, Phys. Rev. B **77**, 214405 (2008).
[8]J. Lindner, I. Barsukov, C. Raeder, C. Hassel, O. Posth, R. Meckenstock, P. Landeros, and D. L. Mills, Phys. Rev. B **80**, 224421 (2009).
[9]R. E. Camley and D. L. Mills, Phys. Rev. B **18**, 4821 (1978).
[10]R. E. Camley, T. S. Rahman, and D. L. Mills, Phys. Rev. B **23**, 1226 (1981).
[11]R. Arias and D. L. Mills, Phys. Rev. B **59**, 11871 (1999).
[12]In the derivation of Eq. (45) of Ref. 11, it has been assumed implicitly that Q is positive definite as one sees from the remarks just below Eq. (34). One needs the form of Eq. (45) for negative Q as well to construct Eq. (14) of the present paper. For general Q the explicit factors of Q on the right-hand side of Eq. (45) are replaced by $|Q|$ [their origin lies in the second term on the left-hand side of Eq. (31)] and the prefactor should be multiplied by $\mathrm{sgn}(Q)$ [when the sign of Q is changed, the sign of the right-hand side of Eq. (31) is changed].
[13]I. Barsukov (private communication).
[14]J. Lindner (private communication).